Structure, Dynamics, and Magnetic Shieldings of Permanganate Ion in Aqueous Solution. A Density Functional Study

Michael Bühl†

Max-Planck-Institut für Kohlenforschung, Kaiser-Wilhelm-Platz 1, D-45470 Mülheim an der Ruhr, Germany

Received: July 3, 2002; In Final Form: September 4, 2002

Car−Parrinello molecular dynamics simulations have been performed for MnO_4^- in the gas phase and in aqueous solution. Dynamic averaging at ca. 300 K affords only minor changes for the mean Mn−O bond length with respect to the optimized value $r_e = 1.622$ Å (BP86 value). Magnetic shieldings, evaluated at the GIAO-B3LYP level for snapshots along the trajectories, decrease upon going from the equilibrium values to the dynamic averages in water. For ^{55}Mn and ^{17}O, the resulting $\sigma^{300K} - \sigma_e$ values amount to −36 and +31 ppm, respectively. The structure of the solvation shell around permanganate ion in water is characterized by the mean number of hydrogen-bonded solvent molecules (approximately 4) and by the g_{MnO} pair correlation function.

Introduction

Contrasting calculated molecular properties with the corresponding experimental observables is a cornerstone of computational chemistry. Owing to the widespread application of NMR spectroscopy, the salient parameters, chemical shifts in particular, play an important role in that respect.[1] This property can be computed with quantum-chemical methods to a good accuracy for a large range of substrates.[2] Typically, the magnetic shieldings are evaluated for isolated molecules in some static structure, obtained either from experiment or from quantum-chemical optimizations. Since the overwhelming majority of experimental NMR spectra are recorded in solution and at ambient temperature, methodological developments on the theoretical side have been extended to account for these conditions. Procedures have been devised to include rovibrational effects in the NMR calculation, for instance by suitable perturbational treatment[3] or by approximating full or partial solutions of the nuclear Schrödinger equation.[4] The popular way to include solvation effects, by way of embedding the molecule in a polarizable continuum, has also been extended to chemical shift calculations.[1,5]

An alternative way to deal with both effects is to perform molecular dynamics (MD) simulations for the substrate embedded in an array of discrete solvent molecules and to average computed magnetic shieldings along the trajectory. Such approaches have been successfully applied to simulate the gas-to-liquid shifts in water[6] and, more recently, to model transition-metal chemical shifts in aqueous solution.[7] For certain iron complexes, for instance, dramatic thermal and solvent effects on $\delta(^{57}Fe)$ have been obtained.[7b]

In a recent validation study for ^{55}Mn chemical shift calculations, it has been noted[8] that the $\delta(^{55}Mn)$ values of organomanganese complexes show systematic deviations from experiment when they are referenced directly to the computed magnetic shielding of isolated, static MnO_4^-, the latter serving as a model for the experimental standard, aqueous $KMnO_4$. It has been speculated that the protic solvent water exerts a stronger effect on the magnetic shielding of the standard than the more inert solvents do on those of the organometallic species.[8] In the present paper an MD study of MnO_4^- in water is presented, calling special attention to thermal and solvent effects on structure and magnetic shieldings of this complex. The resulting effects turn out to be relatively small for ^{55}Mn, but noticeable for ^{17}O. In addition, the simulations afford insights into the structure of the hydration shell around the permanganate ion, an important oxidant in organic and inorganic chemistry.

Computational Details

1. Methods and Basis Sets. The computational methods follow largely those in refs 7a and 8. For species in vacuo, optimizations were performed using the density-functional-based Car−Parrinello scheme[9] as implemented in the CPMD program.[10] The functional combination according to Becke[11] and Perdew[12] was employed (denoted BP86), together with norm-conserving pseudopotentials generated according to the Troullier and Martins procedure[13] and transformed into the Kleinman−Bylander form[14] (see below). Periodic boundary conditions were imposed using a cubic supercell for MnO_4^- (box size 9.8692 Å) and an orthorhombic one for $Mn_2(CO)_{10}$ (box lengths of 14, 14, and 22 Å). Kohn-Sham orbitals were expanded in plane waves up to a kinetic energy cutoff of 80 Ry. The BP86/AE1 geometries from ref 8 were taken as starting points and were reoptimized without symmetry restraints until the maximum gradient was less than 5×10^{-4} au (denoted CP-opt).

$KMnO_4$ stationary points were optimized with the Gaussian 98 program[15,16] at the BP86/AE1 level, that is, using a contracted [9s5p] all-electron Wachters' basis on K[17] (contraction scheme 611111111/33111), a similar [8s5p3d] Wachters' basis,[17] augmented with one diffuse d and two diffuse p sets[18] on Mn (full contraction scheme 62111111/3311111/3111), and 6-31G* basis on O.[19]

For MnO_4^- in vacuo, Car−Parrinello molecular dynamics simulations were performed starting from the equilibrium structure, using a fictitious electronic mass of 600 a.u. and a time step of 0.121 fs. Unconstrained simulations (NVE ensemble) were performed over 1.5 ps at ca. 300 K, the first 0.5 ps of which were taken for equilibration. For aqueous MnO_4^-,

† Fax: 49 + (0)208-306 2996. E-mail: buehl@mpi-muelheim.mpg.de.

10.1021/jp026441h CCC: $22.00
Published on Web 10/12/2002

TABLE 1: Selected Geometrical Parameters (Distances in Angstroms, Angles in Degrees) and Harmonic Vibrational Frequencies (in cm^{-1}) of Two Test Molecules

parameter	CP-opt	BP86/AE1[a]	exptl[b]
	$Mn_2(CO)_{10}$		
r(Mn−Mn)	3.005	2.965	2.977(11)
r(Mn−C_{ax})	1.794	1.812	1.803(16)
r(Mn−C_{eq})	1.861	1.857	1.873(5)
a(C_{ax}−Mn−C_{eq})	93.7	93.8	93.4(5)
	MnO_4^-		
r(Mn−O)	1.622	1.625	1.629 ± 0.005
ν_2 (E)	369	345	360
ν_4 (T_2)	424	392	430
ν_1 (A_1)	979	880	839
ν_3 (T_2)	1049	949	914

[a] Geometries from ref 8. [b] Geometries from refs 23,24, Raman frequencies from ref 25.

the box was filled with 28 water molecules. In order to increase the time step, hydrogen was substituted with deuterium. Simulations started from a well-equilibrated configuration taken from an MD run for $H_2VO_4^-$,[7a] replacing the vanadate with permanganate ion. The system was equilibrated for 0.5 ps maintaining a temperature of 300(±50) K, and was then propagated without constraints for 5ps.

Magnetic shieldings were computed for snapshots along the trajectories employing the B3LYP[20] hybrid functional, together with basis II′, which consists of the same Wachters' basis set on Mn and K as described above and a (9s5p1d)/[5s4p1d] contracted Huzinaga basis on the permanganate O atoms.[21] Snapshots were taken every 25 fs (for gaseous MnO_4^- in addition every 19 fs) over the course of 1 ps. No periodic boundary conditions were employed. For aqueous permanganate, the 10 H_2O molecules nearest to the complex were included specifically, using a double-zeta basis on them (contraction (7s3p)/[4s2p] and (3s)/[2s] for O and H, respectively).[21] These computations were carried out with the Gaussian 98 program package.[15]

2. Validation of the Pseudopotential. For Mn, no well-tested pseudopotential was available, and a semicore (or small-core) pseudopotential was generated corresponding to those used previously for V and Fe.[7a,c,22] Test calculations with this pseudopotential comprised geometry optimizations for MnO_4^- and $Mn_2(CO)_{10}$, and harmonic frequency evaluations for the former. The latter molecule with its Mn-Mn bond was deemed a stringent test case for the quality of the pseudopotential. The resulting parameters are collected in Table 1, together with the corresponding values for nonperiodic all-electron calculations at the BP86/AE1 level and experimental data.[23−25]

The CP-optimized Mn−ligand distances agree within 1−2 pm with the BP86/AE1 or the experimental data. A somewhat larger deviation is found for the CP-optimized Mn−Mn distance in $Mn_2(CO)_{10}$, 3−4 pm (Table 1). This value is probably still acceptable in view of the shallow stretching potential for this bond, as evidenced by the observed shortening (by more than 7 pm) upon going from the gas phase into the crystal.[24] While the harmonic bending modes, evaluated numerically with the CPMD program, agree reasonably well with the corresponding analytical BP86/AE1 values (within 20-30 cm^{-1}, that is), the stretching vibrations are overestimated by ca. 100 cm^{-1}. This value may seem large on a relative basis (10%), but is certainly in the correct order of magnitude, suggesting that the potential energy surface of permanganate is described fairly well, at least qualitatively. Attempts to adjust the Mn pseudopotential such that it would produce improved harmonic frequencies resulted in a deterioration of the optimized geometrical parameters. The adopted pseudopotential thus represents a reasonable compromise and is available from the author upon request.

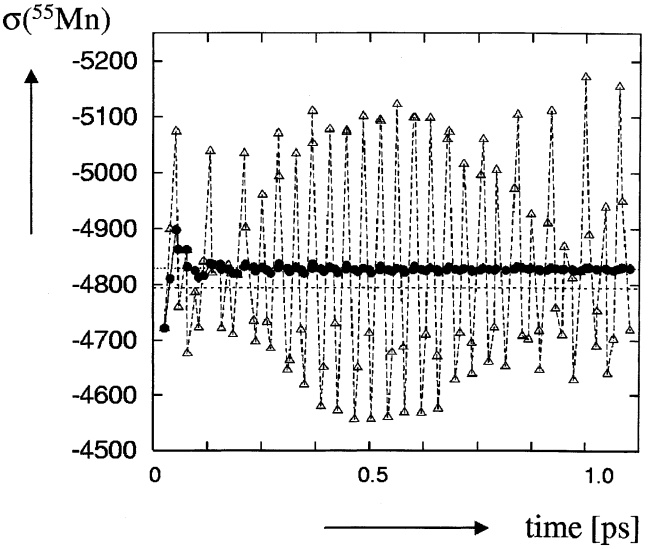

Figure 1. ^{55}Mn magnetic shielding constant (B3LYP/II level) for snapshots from the CPMD trajectory of MnO_4^- in the gas phase. Open triangles: raw data. Filled circles: running average (average value up to this point). Dashed horizontal line: σ_e.

3. Estimation of Rovibrational Corrections. For gaseous MnO_4^-, a one-dimensional Mn−O stretching potential was constructed by performing 11 single-point energy evaluations for different Mn−O distances (T_d symmetry imposed), using the CPMD program and the same setup as that for the geometry optimizations. Spacing of the distances around the equilibrium value, interpolative fit to an analytical Morse function, and numerical solution of the rovibrational Schrödinger equation corresponded to those established in ref 4a. The reduced mass of a single oxygen atom was employed in order to model the symmetrical stretch with a fixed metal center.

Results and Discussion

Simulation in Vacuo. During a 1 ps simulation in the gas phase, the average Mn-O bond length is 1.624(30) Å, only slightly elongated with respect to the equilibrium value r_e = 1.622 Å (Table 1). According to the computed bond-length/shielding derivative $\partial\sigma^{Mn}/\partial r_{MnO}$ = −17000 ppm/Å,[26] this increase in bond distance would correspond to a deshielding of the ^{55}Mn nucleus by 34 ppm. The evolution of the ^{55}Mn shielding constant, evaluated for individual snapshots along the trajectory, is illustrated in Figure 1. The snapshots were taken at two different time intervals in order to avoid accidental coincidence with molecular vibrations.[27] Even though the individual σ(^{55}Mn) values are scattered over a notable range of approximately 500 ppm (open triangles in Figure 1), the running average, that is, the average up to each point, is well converged to within ±1 ppm (solid circles in Figure 1). The mean σ^{300K} value is found to be deshielded with respect to the equilibrium value σ_e by 35 ppm, in excellent accord with the above-mentioned estimate based on the bond-length/shielding derivative.

Quantities averaged over classical MD trajectories do not include zero-point effects, which are purely quantum-mechanical in nature. For magnetic shieldings of lighter nuclei, it has been shown that these zero-point effects can be much larger than the thermal effects on top of them.[3,4] We have argued[7c] that thermal effects on transition-metal magnetic shieldings, evaluated from classical MD, should at least show the correct qualitative trend,

since both classically and quantum-mechanically averaged metal−ligand bond distances would be elongated from their equilibrium values and since it is typically these distances that dominate the metal shieldings.[28] For MnO_4^- in T_d symmetry, one can construct a one-dimensional potential surface, for which the rovibrational Schrödinger equation can be solved precisely. Following the procedure established in reference 4a for diatomics, the resulting zero-point effect for $\delta(^{55}Mn)$, that is, $\sigma^{0K} - \sigma_e$, amounts to −34 ppm, and the total thermal effect at 300 K, $\sigma^{300K} - \sigma_e$, is −36 ppm.

Both of these values are in apparent excellent accord with the CPMD-derived thermal effect given above, $\sigma^{300K} - \sigma_e = -35$ ppm. It must be kept in mind, however, that this degree of agreement is certainly fortuitous, since firstly, the one-dimensional quantum-mechanical picture neglects contributions from the bending and the asymmetric stretching modes, which are of course included in the classical simulation of the real system, and secondly, the temperature dependence of $\sigma(T)$ is markedly different for both approaches.[29] Nevertheless, this one-dimensional model calculation serves to illustrate that the CPMD-based estimate for σ^{300K} is qualitatively correct (deshielded with respect to σ_e), and that it can even be in a reasonable order of magnitude, at least in the present case.[30]

Simulation in Water. When the simulation of MnO_4^- is repeated in a periodic water box, the mean Mn−O bond length (averaged over 5 ps) is 1.621(26) Å, that is, somewhat shorter than the equilibrium value. All optimized and averaged Mn−O distances are in good accord with that of aqueous $KMnO_4$, 1.624 ± 0.005 Å, as estimated from an EXAFS analysis.[31] On the basis of purely geometrical criteria, the average number of water molecules acting as hydrogen-bond donors to permanganate is 3.7.[32] MnO_4^- thus attracts only about half the number of water molecules as the related vanadate $H_2VO_4^-$.[7a] As with the latter, this first solvation shell is not static, but is in dynamic exchange with water molecules from the solvent. Several exchange processes can be monitored during the simulation time. In addition, two intramolecular exchange events were observed, where a hydrogen-bonded water was transferred directly from one metal oxo atom to another, via a transient bifurcated hydrogen bond.

The structure of the solution can be analyzed in terms of suitable pair correlation functions $g(r)$, which are related to the probability of finding two atoms at a given distance.[33] The $g_{MnO}(r)$ function is displayed in Figure 2. Only a very shallow maximum can be discerned around 3.6−3.8 Å ($g = 1.4$), marking the position of the first solvation sphere, and little if any fine structure is apparent beyond that. The $g_{MnO}(r)$ function thus supports the picture of a relatively weakly solvated pemanganate ion. For definite conclusions, a larger box size, longer simulation times and, in particular, inclusion of the counterion would be necessary.

Weak solvation would imply a high reorientational mobility in solution, as described by the molecular correlation time τ_c. For aqueous ND_4^+, a CPMD-based estimate for τ_c has been found to be in the same order of magnitude as the experiment, around 1−2 ps.[34] In the present simulation for MnO_4^-, the ion librates around the initial configuration for most of the time, and only one rotational jump of about 60° is observed after ca. 4 ps (see Figure 3). The limited statistical accuracy due to the short simulation time notwithstanding, this result would suggest a correlation time on the order of several ps, in good qualitative accord with an earlier empirical estimate of 7.4 ps.[35]

What are, finally, the thermal and solvent effects on the chemical shifts? First, it has been tested how the solvent

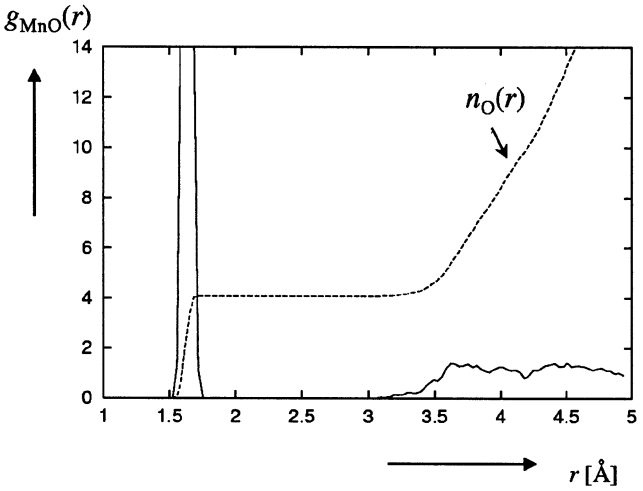

Figure 2. Solid line: simulated manganese−oxygen pair correlation function $g(r)$ in aqueous MnO_4-. Dashed: $n_O(r) = \rho\int g(r)4\pi r^2\,dr$, which integrates to the total number of oxygen atoms in a sphere with radius r around Mn.

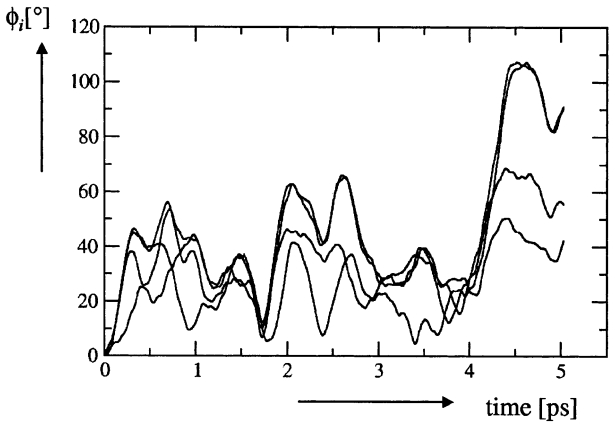

Figure 3. Angles of rotation ϕ_i as a function of simulation time; angles between the initial and the instantaneous orientations of the four MnO bonds are plotted. To integrate out fast and large librational modes, the $\phi_i(t)$ were smoothed over a time interval of 80 fs.

molecules need to be treated in the NMR computations. For $H_2VO_4^-$ it had been shown that it is sufficient to include the surrounding water molecules just as point charges.[7a] For highly charged iron cyanide complexes, on the other hand, this procedure had proven inadequate, and a layer of 20 water molecules had to be treated explicitly.[7b,c] Magnetic shieldings were computed for a representative snapshot consisting of one permanganate ion (II basis) with the 10 nearest water molecules (DZ basis). Subsequent test calculations showed that the computed shieldings change notably when the water molecules are replaced by point charges,[36] and that only minor effects (on the order of a few ppm) are found upon increase of the basis set on the solvent molecules or the number of the latter. Thus, the solvent has to be included specifically, and the number of ten water molecules appeared to be a good compromise between accuracy and computational expense.

On going from the gas phase into water, the correspondingly averaged ^{55}Mn shielding σ^{300K} remains virtually unchanged (compare CPMD and CPMD/H_2O values in Table 2). From the above-mentioned slight Mn-O bond contraction in solution an increased shielding was to be expected. Indeed, when the water molecules were deleted in the NMR snapshots from the solution, affording unsolvated permanganate ions in the geometries of the solvated ones, an averaged σ value of −4776 ppm was

TABLE 2: Computed (GIAO-B3LYP/II) Magnetic Shielding Constants σ of Free and Aqueous MnO_4^-

level of approximation[a]	$\sigma(^{55}Mn)$	$\sigma(^{17}O)$
σ_e//BP86/AE1	−4832	−1094
σ_e//CP-opt	−4794	−1084
σ^{300K}//CPMD	−4829	−1095
σ^{300K}//CPMD/H_2O[b]	−4830	−1053
exptl		−939[c]

[a] Equilibrium and mean σ values, computed or averaged for the geometries obtained as indicated. [b] Averaged for $MnO_4^-\cdot 10H_2O$ clusters taken from the simulation (DZ basis on water in the NMR computations). [c] From ref 40, uncertainty ±8 ppm.

obtained, in line with this expectation. Apparently, indirect solvation effects, arising from the change in geometry, and direct ones, due to the response of the electronic wavefunction, are of similar magnitude, but of opposite direction in this case. As a consequence, a very small net gas-to-liquid shift ensues.

In the previous investigation of (static) ^{55}Mn chemical shifts it had been noted that systematic deviations from experiment occur when the computed magnetic shieldings are referenced directly to the one obtained for MnO_4^-.[8] At the GIAO-B3LYP level, for instance, the resulting $\delta(^{55}Mn)$ values were too strongly shielded by ca. 300 ppm. It is clear from the present study that thermal and solvation effects on the permanganate ion cannot account for discrepancies this large. In fact, since these effects turn out to be unusually small for MnO_4^-, it might be possible that they are considerably larger for the other organomanganese substrates studied in reference 8. Further theoretical work should be expended along this line.

The present study of aqueous MnO_4^- neglects the effect of the counterion. Inclusion of the latter, for instance in form of aqueous K^+, would in principle be possible.[37] For solvent-separated ion pairs, however, a very large counterion effect on $\sigma(^{55}Mn)$ would seem unlikely because the ions would be too far apart. Only for contact ion pairs a large such effect would seem possible. But even for an isolated $KMnO_4$ molecule, the computed $\delta(^{55}Mn)$ relative to free MnO_4^- was less than 50 ppm (for the most stable C_{2v} symmetric minimum with two K···O contacts). Thus, no simulation with explicit inclusion of a counterion was deemed necessary.[38]

The ^{17}O magnetic shieldings are included in Table 2. This property has been studied previously[39] in order to assess the quality of the density functional employed in the NMR calculations. Pure density functionals (GGAs) and hybrid variants have been found, respectively, to over- and underestimate $\sigma(^{17}O)$ to a similar extent (on the order of 100−150 ppm). For instance, employing the GIAO-B3LYP method and the isolated, CP-opt structure, $\sigma = -1084$ is computed, which is too strongly deshielded by 155 ppm with respect to experiment (Table 2). The experimental value refers to aqueous solution, presumably at ambient temperature.[40] Thermal averaging in the gas phase affords an additional, small deshielding by 11 ppm (compare CP-opt and CPMD values in Table 2). Immersion in water leads to a notable shielding of the ^{17}O nucleus, with a predicted gas-to-liquid shift of 42 ppm (−42 ppm on the δ scale), similar to that of ^{17}O in water. The resulting difference $\sigma_e - \sigma^{300K}$ thus amounts to 31 ppm. Correction by this value of the B3LYP permanganate ^{17}O shieldings[39] thus improves the accord with experiment.

Finally, it should be noted that the computed thermal and solvent effects on $\sigma(^{17}O)$ are larger on a relative basis than those on $\sigma(^{55}Mn)$, since the chemical shift range of the metal (ca. 3000 ppm) exceeds that of ^{17}O (ca. 1900 ppm).

Conclusions

Thermal and solvent effects on structural and NMR parameters of permanganate ion were probed by means of density-functional based molecular dynamics simulations. For the pristine ion in the gas phase at ca. 300 K, a slight elongation of the mean MnO bond length with respect to the equilibrium value is found. The concomitant deshielding of the ^{55}Mn nucleus, on the order of ca. 35 ppm, is very similar when obtained either from a classical description of the full molecular dynamics, or from a quantum-mechanical treatment of a single degree of freedom, namely the MnO stretch. Immersion in aqueous solution, modeled by placement in a periodic box containing 30 water molecules, results in a very small contraction of the mean MnO bond length. On going from the equilibrium magnetic shieldings to the averaged values in solution, ^{55}Mn and ^{17}O nuclei are deshielded and shielded, respectively, by approximately 35 ppm. For the metal with its large chemical-shift range, this is a relatively small value, which cannot account for systematic deviations of ^{55}Mn chemical shifts found upon direct referencing to permanganate. For ^{17}O, the computed shielding upon solvation improves the accord of experiment with theoretical results obtained using hybrid density functionals.

The simulations in water reveal interesting details of the solvation shell around aqueous permanganate. Solvation is not very strong, as assessed by the mean number of hdrogen-bonded solvent molecules, which is less than four, and by the absence of distinct maxima in the MnO pair correlation function. This should be reflected in a high rotational mobility, quantitative assessment of which, however, is hampered by the short simulation time of 5 ps. From a single observed ≈60° jump, a molecular correlation time on the picosecond time scale can be estimated. Further studies are in progress, which are aimed at unraveling the effects of thermal averaging and solvation on transition metal chemical shifts.

Acknowledgment. The author wishes to thank Prof. W. Thiel for his continuing support, the Deutsche Forschungsgemeinschaft for a Heisenberg fellowship, Prof. M. Parrinello and coworkers for assistance with the CPMD program, Dr. Th. Heine, Prof. H. Huber, and Prof. V. G. Malkin for helpful discussions, as well as Prof. D. Sundholm for a copy of his program to solve the rovibrational Schrödinger equation. Computations were performed on Compaq XP1000 and ES40 workstations at the MPI Mulheim and on a Hitachi-SR8000 at the Leibniz Rechenzentrum in Munich.

References and Notes

(1) See for instance: Cremer, D. Olsson, L.; Reichel, F.; Kraka, E. *Isr. J. Chem.* **1993**, *33*, 369−385.

(2) For selected reviews, see: (a) Helgaker, T.; Jaszunski, M.; Ruud, K. *Chem. Rev.* **1999**, *99*, 293−352. (b) Bühl, M.; Kaupp, M.; Malkin, V. G.; Malkina, O. L. *J. Comput. Chem.* **1999**, *20*, 91−105.

(3) (a) Ruud, K.; Åstrand, P.-O.; Taylor, P. R. *J. Chem. Phys.* **2000**, *112*, 2668−2683. (b) Ruud, K.; Åstrand, P.-O.; Taylor, P. R. *J. Am. Chem. Soc.* **2001**, *123*, 4826−4833.

(4) For instance: (a) Sundholm, D.; Gauss, J.; Schäfer, A. *J. Chem. Phys.* **1996**, *105*, 11051−11059. (b) Fukui, H.; Baba, T.; Narumi, H.; Miura, K.; Matsuda, H. *J. Chem. Phys.* **1996**, *105*, 4692−4699. (c) Cromp, B.; Carrington, T., Jr.; Salahub, D. R.; Malkina, O. L.; Malkin, V. G. *J. Chem. Phys.* **1999**, *110*, 7153−7159. (d) Jordan, M. J. T.; Toh, J. S.-S.; Del Bene, J. E. *Chem. Phys. Lett.* **2001**, *346*, 288−292. (e) Böhm, M. C.; Schulte, J.; Ramírez, R. *Int. J. Quantum. Chem.* **2002**, *86*, 280−296.

(5) (a) Mennucci, B.; Martínez, J. M.; Tomasi, J. *J. Phys. Chem. A* **2001**, *105*, 7287−7296. (b) Vreven, T.; Mennucci, B.; da Silva, C. O.; Morokuma, K.; Tomasi, J. *J. Chem. Phys.* **2001**, *115*, 62−72. (c) Yamazaki, T.; Sato, H.; Hirata, F. *J. Chem. Phys.* **2001**, *115*, 8949−8957.

(6) (a) Malkin, V. G.; Malkina, O. L.; Steinebrunner, G.; Huber, H. *Chem. Eur. J.* **1996**, *2*, 452−457. (b) Pfrommer, B. G.; Mauri, F.; Louie,

S. G. *J. Am. Chem. Soc*. **2000**, *122*, 123−129. (c) Sebastiani, D.; Parrinello, M. *J. Phys. Chem. A* **2001**, *105*, 1951−1958.

(7) (a) Bühl, M.; Parrinello, M., *Chem. Eur. J.* **2001**, *7*, 4487−4494. (b) Bühl, M.; Mauschick, F. T.; Terstegen, F.; Wrackmeyer, B. *Angew. Chem., Int. Ed.* **2002**, *41*, 2312−2315. (c) Bühl, M.; Mauschick, F., *Phys. Chem. Chem. Phys*, in press.

(8) Bühl, M. *Theor. Chem. Acc*. **2002**, *107*, 336−342.

(9) Car, R.; Parrinello, M. *Phys. Rev. Lett*. **1985**, *55*, 2471−2474.

(10) Hutter, J.; Alavi, A.; Deutsch, T.; Bernasconi, M.; Goedecker, S.; Marx, D.; Tuckerman, M.; Parrinello, M. CPMD, version 3.3a; Max-Planck-Institut für Festkörperforschung and IBM Research Laboratory (1995−1999).

(11) Becke, A. D. *Phys. Rev. A* **1988**, *38*, 3098−3100.

(12) Perdew, J. P. *Phys. Rev. B* **1986**, *33*, 8822−8824. Perdew, J. P. *Phys. Rev. B* **1986**, *34*, 7406.

(13) Troullier, N.; Martins, J. L. *Phys. Rev. B* **1991**, *43*, 1993−2006.

(14) Kleinman, L.; Bylander, D. M. *Phys. Rev. Lett*. **1982**, *48*, 1425−1428.

(15) Frisch, M. J.; Trucks, G. W.; Schlegel, H. B.; Scuseria, G. E.; Robb, M. A.; Cheeseman, J. R.; Zakrzewski, V. G.; Montgomery, J. A.; Stratman, R. E.; Burant, J. C.; Dapprich, S.; Millam, J. M.; Daniels, A. D.; Kudin, K. N.; Strain, M. C.; Farkas, O.; Tomasi, J.; Barone, V.; Cossi, M.; Cammi, R.; Mennucci, B.; Pomelli, C.; Adamo, C.; Clifford, S.; Ochterski, J.; Petersson, G. A.; Ayala, P. Y.; Cui, Q.; Morokuma, K.; Malick, D. K.; Rabuck, A. D.; Raghavachari, K.; Foresman, J. B.; Cioslowski, J.; Ortiz, J. V.; Baboul, A. G.; Stefanov, B. B.; Liu, C.; Liashenko, A.; Piskorz, P.; Komaromi, I.; Gomperts, R.; Martin, R. L.; Fox, D. J.; Keith, T.; Al-Laham, M. A.; Peng, C. Y.; Nanayakkara, A.; Gonzalez, C.; Challacombe, M.; Gill, P. M. W.; Johnson, B. G.; Chen, W.; Wong, M. W.; Andres, J. L.; Gonzales, C.; Head-Gordon, M.; Replogle, E. S.; Pople, J. A. Gaussian 98; Gaussian, Inc.: Pittsburgh, PA, 1998.

(16) This species was optimized with Gaussian rather than with the CPMD program because no well-tested pseudopotential for K was available to be used with the latter in conjunction with BP86. In any event, only small differences between all-electron and plane-wave/pseudopotential results are to be expected in this case.

(17) Wachters, A. J. H. *J. Chem. Phys.* **1970**, *52*, 1033−1036.

(18) Hay, P. J. *J. Chem. Phys.* **1977**, *66*, 4377−4384.

(19) (a) Hehre, W. J.; Ditchfield, R.; Pople, J. A. *J. Chem. Phys.* **1972**, *56*, 2257−2261 (b) Hariharan, P. C.; Pople, J. A. *Theor. Chim. Acta* **1973**, *28*, 213−222.

(20) Lee, C.; Yang, W.; Parr, R. G. *Phys. Rev. B* **1988**, *37*, 785−789.

(21) Kutzelnigg, W.; Fleischer, U.; Schindler, M. In *NMR Basic Principles and Progress*; Springer-Verlag: Berlin, 1990; Vol. 23, pp 165−262.

(22) The cutoff radii used for the s-, p-, and d-channels were 2.0, 2.1, and 1.5 au, respectively; see also Bachelet, G. B.; Hamann, D. R.; Schlüter M. *Phys. Rev. B* **1982**, *26*, 4199−4228.

(23) X-ray $KMnO_4$: Palenik, J. G. *Inorg. Chem*. **1967**, *6*, 503−507.

(24) (a) GED $Mn_2(CO)_{10}$: Almenningen, A., Jacobsen, G. G.; Seip, H., M. *Acta Chem. Scand.* **1969**, *23*, 685−686. (b) X-ray: Bianchi, R.; Gervasio, G.; Marabello, D. *Inorg. Chem*. **2000**, *39*, 2360−2366.

(25) Raman data for aqueous $KMnO_4$: Weinstock, N.; Schulze, H.; Müller, A. *J. Chem. Phys.* **1973**, *59*, 5063−5067.

(26) Obtained by a linear fit of GIAO-B3LYP/II ^{55}Mn shielding constants for four different T_d symmetric structures with Mn−O distances spaced around r_e.

(27) The Mn−O stretching frequencies around 1000 cm^{-1} correspond to a vibrational period of ca. 33 fs, sufficiently different from the chosen snapshot intervals. Another indicator for the absence of artifacts due to a given interval is the Mn−O distance averaged over the respective snapshots, which in both cases is identical to the average over the whole trajectory.

(28) Also see: (a) Leitner, W.; Bühl, M.; Fornika, R.; Six, C.; Baumann, W.; Dinjus, E.; Kessler, M.; Krüger, C.; Rufinska, A. *Organometallics* **1999**, *18*, 1196−1206. (b) Donkervoort, J. G.; Bühl, M.; Ernsting, J. M.; Elsevier: C. J. *Eur. J. Inorg. Chem*. **1999**, 27−33.

(29) No CPMD simulations were performed for other temperatures, but it is clear that, in a classical simulation, $\sigma^{0K} - \sigma_e$ must be zero and that, consequently, in the range between 0 and 300 K the averaged magnetic shielding σ^T would change much more steeply in the classical than in the quantum-mechanical simulation.

(30) The same result was found for another test calculation, namely for F_2: The $\sigma^{300K} - \sigma_e$ values obtained from the CPMD/BLYP-based average and from solving the Schrödinger equation of the corresponding CP/BLYP potential surface are −21 and −19 ppm, respectively (GIAO-B3LYP shieldings). The discrepancy from the values given in ref 4c and 4a for F_2, −27 and −36 ppm, respectively, is due to the different potential and shielding surfaces employed there, which were based on nonhybrid DFT and CCSD(T) calculations, respectively.

(31) Sham, T. K.; Brunschwig, B. S. *J. Am. Chem. Soc.* **1981**, *103*, 1590−1591.

(32) From structural considerations (fitting into a polyhedral model of bulk water), a higher coordination number has been estimated, namely, 6+2: Lyashchenko, A. K. In *Relaxation Phenomena in Condensed Matter (Adv. Chem. Phys.* Vol. 87), Coffey, W., Ed.; Wiley: New York, 1994; pp 379−426.

(33) For the definition of the pair correlation function, for example, see: Allen, M. P.; Tildesley, D. J. *Computer Simulation of Liquids*; Clarendon Press: Oxford, 1987.

(34) Brugé, F.; Bernasconi, M.; Parrinello, M. *J. Am. Chem. Soc*. **1999**, *121*, 10883−10888.

(35) Kidd, R. G. *J. Magn. Reson.* **1981**, *45*, 88−93.

(36) Charges from natural population analysis (BP86/6-31G* level) for a single water molecule.

(37) For a CPMD study of aqueous K^+ using the BLYP functional see: Ramaniah, L. M.; Bernasconi, M.; Parrinello, M. *J. Phys. Chem.* **1999**, *111*, 1587−1591.

(38) Also, a meaningful description of a solvens-separated ion pair would probably require a much longer simulation time, as the reorientation of solvated ions with respect to each other would happen on a larger time scale than a few picoseconds that can be simulated at present.

(39) (a) Kaupp, M.; Malkina, O. L.; Malkin, V. G. *J. Chem. Phys*. **1997**, *106*, 9201−9212. (b) Wilson, P. J.; Amos, R. D.; Handy, N. C. *Phys. Chem. Chem. Phys*. **2000**, *2*, 187−194.

(40) Figgis, B. N.; Kidd, R. G.; Nyholm, R. S. *Proc. Chem. Soc. A* **1962**, *269*, 469−480; the $\delta(^{17}O)$ value given there was converted to the absolute shielding scale using the $\sigma(^{17}O)$ value of $H_2O(l)$ as employed in ref 39.